J Solid State Electrochem (2008) 12:575–581
DOI 10.1007/s10008-007-0335-z

ORIGINAL PAPER

Selective electrocatalysis of acetaldehyde oxime reduction on (111) sites of platinum single crystal electrodes and nanoparticles surfaces

P. Rodríguez · E. Herrero · J. Solla-Gullón · J. M. Feliu · A. Aldaz

Received: 24 August 2006 / Revised: 27 January 2007 / Accepted: 30 January 2007 / Published online: 19 June 2007

Abstract The reduction of acetaldehyde oxime (AO) in acid medium on platinum surfaces is a structure sensitive reaction that takes place almost exclusively on (111) sites of Pt electrodes, and it is strongly inhibited on Pt(100) and Pt (110) surfaces. A study using stepped electrodes with (111) terraces and monoatomic steps either with (100) and (110) orientation shows that the activity of the electrode is also dependent on the terrace width, i.e., the wider the terrace is, the higher current density is recorded and the more positive the peak potential for AO reduction appears. Moreover, in the electrodes with (100) step sites, the reduction process appears at more negative potential than the electrodes with (111) step sites. Nanoparticles with some preferential orientations were also tested for the AO reduction reaction to check the presence of (111) ordered domains on the nanoparticles surface.

Keywords Acetaldehyde oxime reduction · Stepped surfaces · Structure sensitive reaction · Platinum single crystal · Platinum nanoparticles

Dedicated to Teresa Iwasita on the occasion of her retirement and for her contributions to Electrochemistry.

P. Rodríguez · E. Herrero (✉) · J. Solla-Gullón · J. M. Feliu · A. Aldaz
Departamento de Química Física, Instituto de Electroquímica, Universidad de Alicante,
Apdo. 99,
03080 Alicante, Spain
e-mail: herrero@ua.es

Introduction

One of the key parameters governing the reaction rate of electrocatalytic reactions is the electrode surface structure. Single crystal electrochemistry has revealed that some of the most important electrochemical reactions are structure sensitive. In fact, the reaction rate can be increased significantly by using the appropriate electrode. Methanol, formic acid, carbon monoxide, and ammonia oxidation are clear examples of such reactions [1–10]. On the other hand, real catalysts are made of nanoparticles, which are basically polycrystalline. Being the surface structure so important for most of the electrode reactions, the surface structure should be tailored to maximize their catalytic activity by developing methods to prepare platinum nanoparticles with preferential orientation [11–13]. This strategy tries to optimize the shape of the nanoparticles to achieve the maximum catalytic activity with the minimum load of the precious metal.

Recently, it has been shown that the reduction of acetaldehyde oxime (AO; $CH_3CH{=}NOH$) takes place on Pt(111) electrodes in the region where hydrogen adsorption takes place [14]. Additionally there are some indications that the reduction of AO can be very sensitive to the surface structure of the electrode. This oxime has to be regarded as an aldoxime because the N–OH functional group is terminal. The electrolytic reduction yields the corresponding amine at Hg or Pb and proceeds by a transference of one electron and one proton at the metal surface as proposed in various Albery's papers [15]. In the presence of adsorbed hydrogen on Raney nickel or on platinum electrodes, the chemically driven hydrogenation reaction can take place.

The reduction process involves the transference of four electrons in consecutive steps simplified as follows [15]:

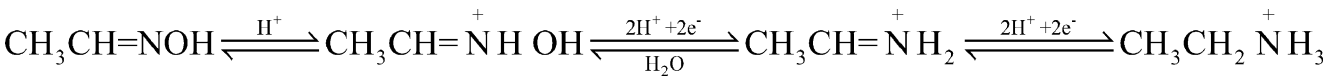

In this manuscript, the reduction of AO will be studied on different platinum single crystal electrodes, namely, low index planes and stepped surfaces, to study the dependence of the reduction reaction on the electrode surface structure. These results will help to understand the reactivity for AO reduction of different platinum nanoparticle electrodes, in which the shape of the nanoparticles has been deliberately tailored.

Materials and methods

Platinum single crystals were oriented, cut, and polished from small single crystal beads (2.5 mm diameter) by the procedure described previously [16]. The surfaces used were Pt(111) itself and those belonging to the series Pt(S)[n−1(111)×(110)] having Miller indices Pt(n,n,n−2) and Pt(S)[n(111)×(100)] surfaces, which have Miller indices Pt(n+1,n−1,n−1). As usual, n represents the number of terrace atoms. The electrodes were flame-annealed and cooled down in a H_2+Ar atmosphere in the usual way. It has been shown that this procedure leads to surface topographies reasonably close to the nominal ones [17, 18].

The nominal step density of these electrodes is defined by the following equations:

$$N_{(111)\times(111)} = \frac{2}{\sqrt{3}d\left(n-\frac{2}{3}\right)} \quad (1)$$

for the Pt(n,n,n−2) surfaces and

$$N_{(111)\times(100)} = \frac{2}{\sqrt{3}d\left(n-\frac{1}{3}\right)} \quad (2)$$

for the Pt(n+1,n−1,n−1) surfaces. In these equations, d is the platinum atomic diameter and is equal to 0.278 nm.

A single crystal platinum bead obtained by fusion of a Pt wire was used as a polycrystalline surface. For the study of this electrode, the crystal bead fully immersed in the cell solution was also used as a reproducible form of a polyoriented platinum electrode having a uniform distribution of all surface sites (i.e., a polycrystalline platinum electrode).

Preferentially oriented nanoparticles were prepared by using a so-called colloidal method [19, 20]. In brief, a variable amount of sodium polyacrylate (PA) solution was added to a 100 ml of an aged 1×10^{-4} M solution containing the desired Pt precursor. Thus, K_2PtCl_4 was employed for the synthesis of the "(100)" nanoparticles, whereas H_2PtCl_6 was used to prepare the "(111)" nanoparticles. After 20 min of Ar bubbling, the Pt ions were reduced by bubbling H_2 for 5 min. The reaction vessel was then sealed, and the solution was left overnight. After complete reduction (12–24 h), two NaOH pellets were added to produce the precipitation of the nanoparticles. After complete precipitation, the nanoparticles were washed two to three times with ultra-pure water. The shape and size of the nanoparticles were determined by transmission electron microscopy (TEM), whereas, the fraction of (111) and (100) ordered domains in the nanoparticle surface were estimated using the irreversible adsorption of bismuth and germanium as previously reported [21–23].

Experiments were carried out at room temperature, 20 °C, in classical two-compartment electrochemical cells deaerated for 20 min by bubbling Ar (N50, Air Liquide in all gases used), including a platinum counterelectrode and a reversible hydrogen (N50) electrode (RHE) as reference. Solutions were prepared from sulfuric acid (doubly distilled, Aldrich), AO 99% from Aldrich and ultrapure water from Elga. The cleanliness of the solutions was tested by the stability of the characteristic voltammetric features of well-defined Pt(111) electrodes.

Results and discussion

In a paper devoted to fundamental aspects related to the potential of zero total charge of platinum electrodes, Pierozynski and Conway [14] reported that the Pt(111) electrode has a significant activity for the reduction of AO. As shown in Fig. 1, the reduction of the oxime takes place in the region where hydrogen adsorption occurs. When compared to the voltammetric profile in the absence of oxime in the same supporting electrolyte, significant differences are observed in the whole potential window. The absence of the characteristic spike at 0.45 V and the hump at 0.71 V, both associated to surface processes in the bisulfate adlayer on the Pt(111) electrode, indicates that the oxime is adsorbed on the electrode surface, preventing the adsorption of bisulfate. In the negative scan direction, the reduction of the adsorbed molecule starts at 0.28 V, giving rise to a well-

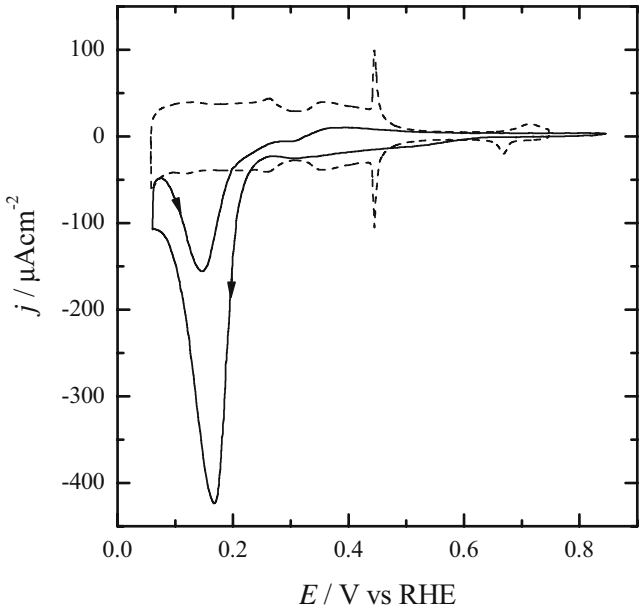

Fig. 1 Voltammetric profiles of Pt(111) electrode in 0.5 M H_2SO_4 in absence (*broken lines*) and presence of 0.01 M AO (*solid line*). Scan rate: 50 mV s^{-1}

marked peak at 0.165 V. The charge transferred in the whole reduction process is much higher than that corresponding to the reduction of a single monolayer, which suggests that the reduction process is not restricted to a single layer of adsorbed molecules. When an adsorbed molecule is reduced, a new molecule replaces it on the surface, and the reduction continues. However, the reduction peak was not the typical shape associated to a process controlled by the diffusion of the reactant to the surface, indicating that the adsorption process controls the rate of the reduction reaction. As hydrogen is absorbed on a bare Pt(111) electrode in this potential region, competitive adsorption between the oxime and hydrogen may take place. This situation is found at potentials negative to the peak; the diminution in the reduction current can be then associated to the displacement of the adsorbed oxime molecules due to the competitive adsorption of hydrogen in this potential region, in a similar way to other cases [24, 25]. Although AO reduction is not completely suppressed at the onset for hydrogen evolution, the difference in the currents measured at 0.08 V between the positive and negative scans at 50 mV/s is ca. 60 μA cm^{-2}, the same value as that obtained in absence of the oxime in solution and associated to the pseudo-capacitive process of hydrogen adsorption/desorption. This fact suggests that the amount of oxime adsorbed at this potential is negligible. Therefore, the diminution in the current below 0.165 V can be ascribed to the desorption of the molecule forced by hydrogen adsorption. In the positive scan, reduction currents are also observed, in the same potential region. However, the maximum current measured in the positive scan is significantly smaller than that of the negative scan, a clear indication that the surface is probably poisoned by some intermediate species generated in the reduction process.

It is important to indicate that the voltammetric profile changes upon the cycling (Fig. 2). The reduction current for the negative and positive scans diminishes significantly, and the peak potential is shifted towards positive values. Moreover, a new voltammetric peak appears at 0.3 V. These effects are probably associated to the accumulation on the surface of several reaction intermediates or by-products, all containing nitrogen groups. It is well known that organic molecules with nitrogen groups are strongly adsorbed on the platinum electrodes [26–28]. The presence of these molecules on the electrode surface modifies the electrode reactivity, diminishing the reduction currents and giving rise to a new peak associated to their reduction. Moreover, these adsorbed molecules prevent the reduction of additional AO molecules on the positive scan, as observed for the third to sixth cycle. Previous reports indicate that the reduction of the AO, unlike the formaldehyde oxime, did not give rise to a significant formation of poisoning species, and the voltammetric profile did not change upon cycling [14]. The difference with these results is probably related to the difference in oxime concentration used (5×10^{-4} vs 0.05 M in this study). Higher oxime concentrations favor the formation and accumulation of reaction intermediates and by-products on the electrode surface. These observations suggest that AO reduction follows complex kinetics, whose study is beyond the scope of this paper. In the following, only the first cycle after the annealing of the electrode will be considered to try to minimize the role of adsorbed residues in the whole process.

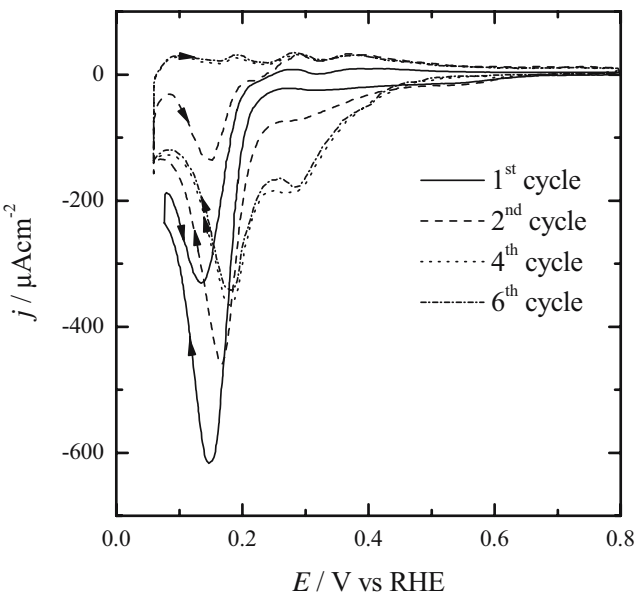

Fig. 2 Successive voltammetric profiles of the Pt(111) electrode in 0.5 M H_2SO_4+5×10^{-2} M AO. Scan rate: 50 mV s^{-1}

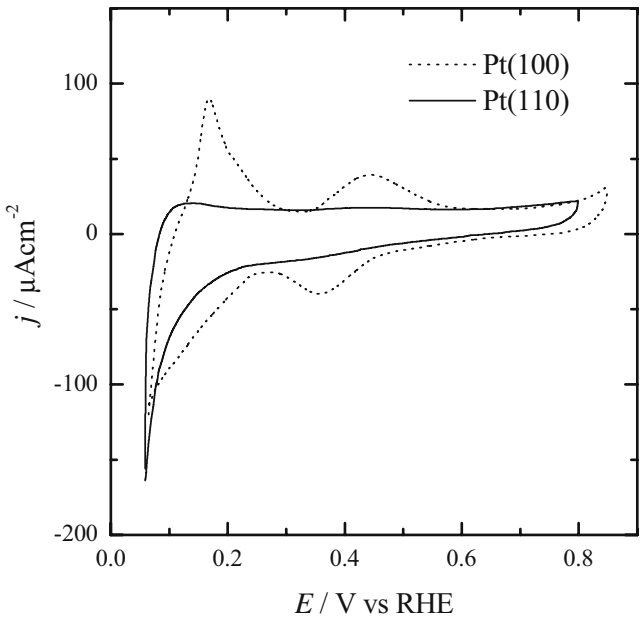

Fig. 3 Voltammetric profiles of Pt(110) and Pt(100) electrodes in 0.5 M H_2SO_4+0.01 M AO. Scan rate: 50 mV s^{-1}

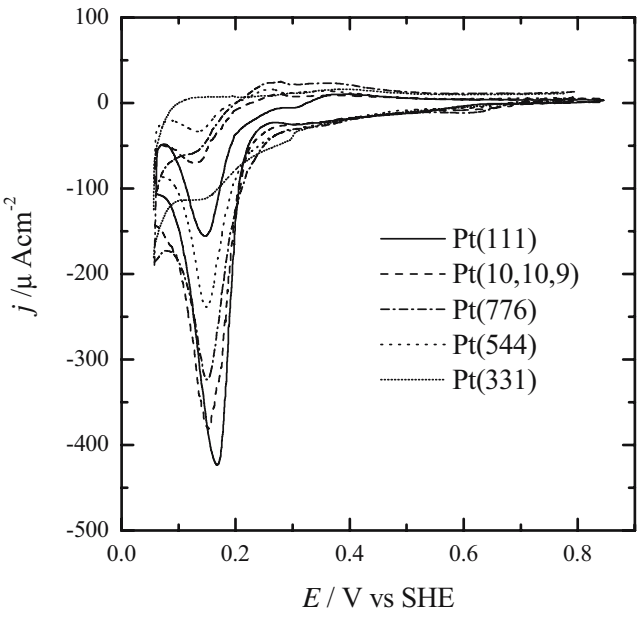

Fig. 4 Voltammetric profiles of the Pt(n,n,n–2) electrodes in 0.5 M H_2SO_4+0.01 M AO. Scan rate: 50 mV s^{-1}

Interestingly, Pt(111) electrodes show a significant activity for the reduction of the oxime. On the other hand, almost negligible reduction currents were observed for the other two basal electrodes (Fig. 3). For Pt(110) and Pt(100) electrodes, the voltammetric profile does not show significant reduction currents and has the typical shape of fully blocked electrode, a clear indication that oxime is strongly adsorbed on the electrode surface. This is especially evident in the case of Pt(110), which only shows a small current at potentials lower than 0.13 V. For higher potentials, the voltammogram is featureless, a consequence of the lack of reactivity of the adsorbed oxime layer on this electrode. For the Pt(100) electrode, two pairs of oxidation–reduction peaks are observed at around 0.39 and 0.16 V. However, these peaks are probably limited to the adsorbed layer, as the charge measured in the positive and negative scans are very similar.

As Fig. 3 suggests, the reduction of the oxime is extremely sensitive to the presence of (111) sites, as in the other basal planes, having ideally only (100) or (110) sites, the only process observed are related to the adsorption of the molecule. To confirm that hypothesis, the reduction of the oxime on stepped surfaces containing (111) terraces and monoatomic steps with (111) and (100) symmetry was studied.

The AO reduction in stepped surfaces with symmetry Pt (s)[n(111)×(111)] and Miller index Pt(n,n,n−2) is shown in Fig. 4. For comparison, the Pt(111) electrode was also included. As can be seen, AO reduction is very sensitive to the width of (111) domains. The main peak current density diminishes, and the peak potential shifts towards negative potential values as the terrace length diminishes. However, the onset for the oxime reduction is shifted slightly toward positive potentials. All these changes are consequence of the terrace width diminution. We can propose that for narrower terraces, the oxime adlayer formed at positive potentials is less compact or has higher number of defects, and therefore, it is easily reduced. For that reason, the onset is shifted towards positive potentials. Once the reduction has started, the currents obtained are always lower than those measured on the Pt(111), as the number of (111)

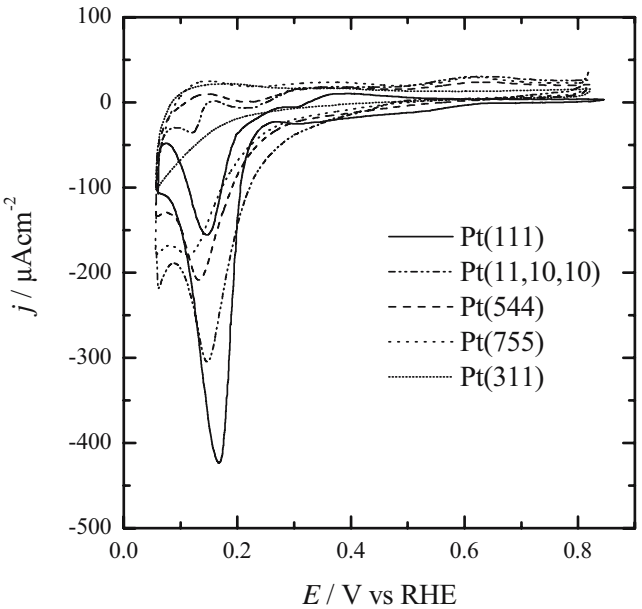

Fig. 5 Voltammetric profiles of the Pt(n+1,n−1,n−1) electrodes in 0.5 M H_2SO_4+0.01 M AO. Scan rate: 50 mV s^{-1}

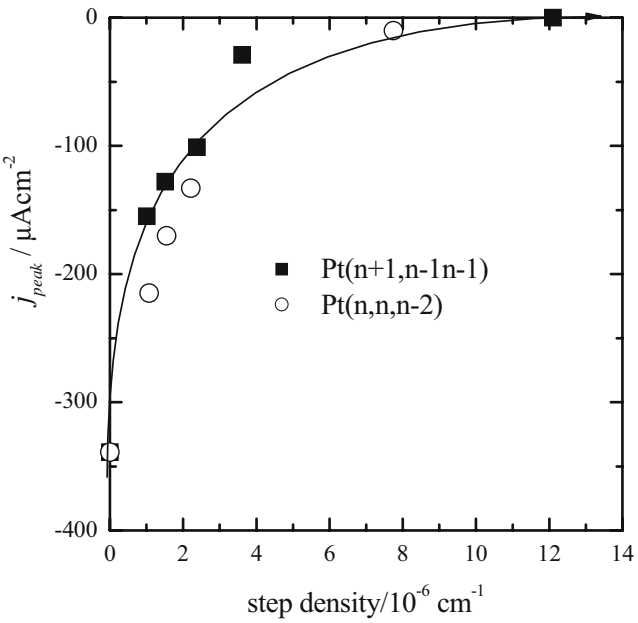

Fig. 6 Peak currents for AO reduction after baseline correction for the Pt(n,n,$n-2$) and Pt($n+1$,$n-1$,$n-1$) electrodes vs step density

terrace sites, which are the most active for the oxime reduction, diminishes. In this case, some ensemble effects cannot be discarded, i.e., the oxime reduction seems to require more than a single site for its reduction, as the current measured for the Pt(311) (surface with two atom-wide terraces) is almost negligible. The displacement of the reduction peak towards negative potentials can be associated with the effect of the terrace width in the hydrogen

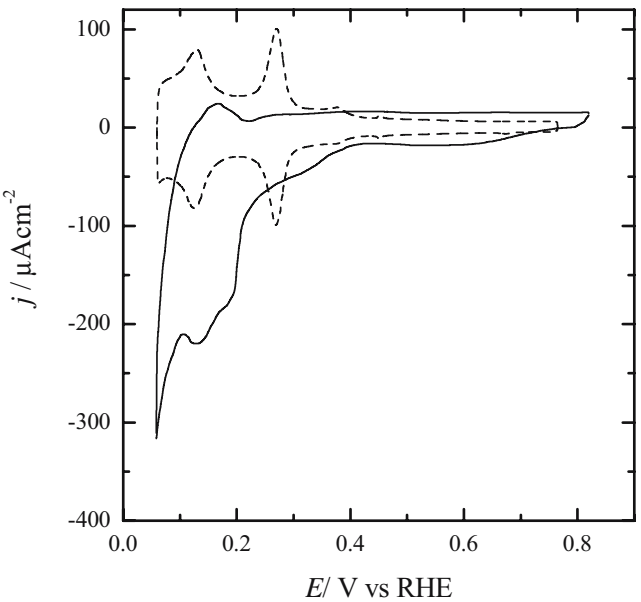

Fig. 7 Voltammetric profiles of a polyoriented Pt single crystal electrode in 0.5 M H_2SO_4 (*broken lines*) and 0.5 M H_2SO_4+0.01 M AO (*solid line*). Scan rate: 50 mV s^{-1}

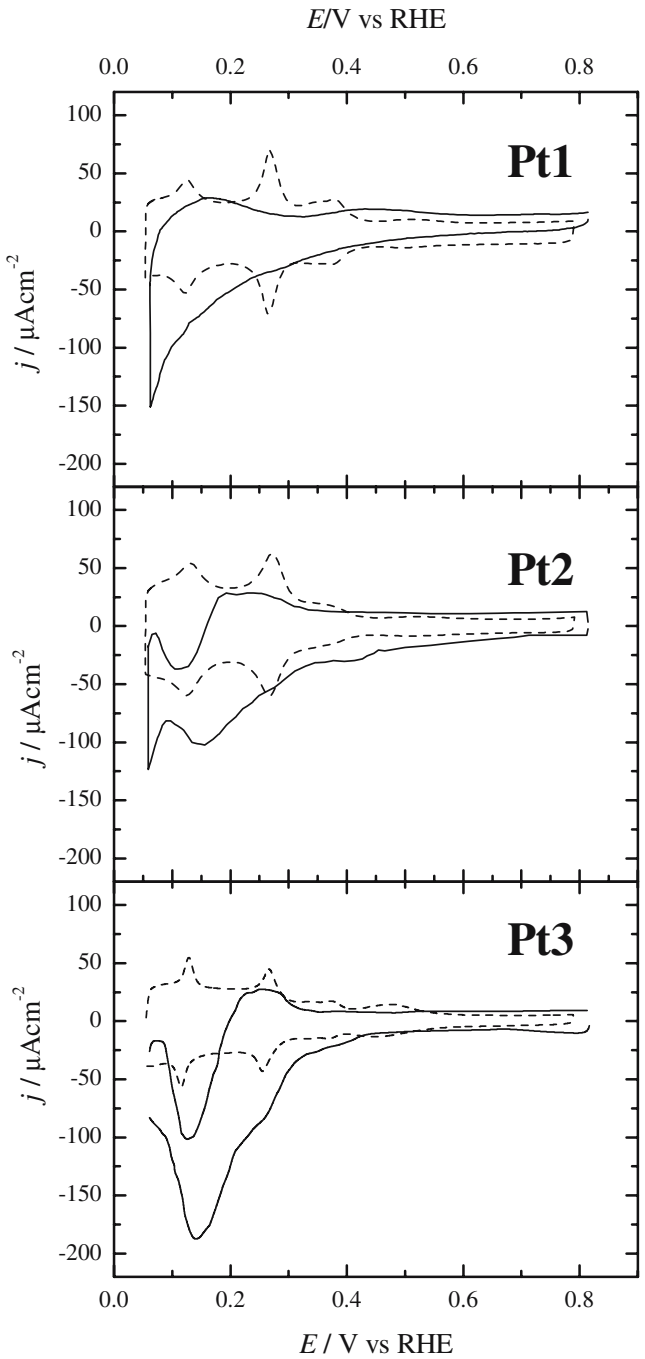

Fig. 8 AO reduction on the different nanoparticles samples in 0.5 M H_2SO_4 (*broken lines*) and 0.5 M H_2SO_4+0.01 M AO (*solid line*). Scan rate: 50 mV s^{-1}

Table 1 Percentage of (100) and (111) terrace sites on the different samples measured with bismuth and germanium adsorption procedures

	Mean size	(111) sites	(100) sites
Pt1	9±3 nm	15	73
Pt2	9±3 nm	22	32
Pt3	9±3 nm	40	32

adsorption. For the narrower terraces, the hydrogen adsorption processes are also shifted towards negative potentials [29], and consequently, the replacement of the oxime from the surface by the adsorbing hydrogen is also shifted negatively. Another important feature that is very sensitive to the terrace width is the reduction current measured in the positive scan between 0.1 and 0.3 V. In the positive scan direction, only significant currents are measured for the surfaces with wide terraces, for which a reduction peak is clearly visible. The differences in the currents measured in the positive and negative scans direction are probably associated to the accumulation of by-products on the electrode surface, which act as poison for the main reduction reaction.

A similar tendency was observed for the AO reduction in stepped surfaces with symmetry Pt(s)[n(111)×(100)] and Miller index Pt(n+1,n−1,n−1) shown in Fig. 5. The main peak current density diminishes, and the peak potential shifts to more negative potential values as the terrace length diminishes. Although the qualitative behavior is the same as that reported for the other series of stepped surfaces, some differences are observed when comparing surfaces with the same terrace width and different step symmetry. The peak potential for the surfaces with (100) steps appears at slightly more negative potentials, although peak currents are similar, suggesting some influence of the step symmetry on the adsorption process of the oxime.

Peak currents for the AO reduction have been plotted in Fig. 6. As aforementioned, peak currents diminish as the step density increases. If AO reduction had required only one (111) terrace site, a linear dependence between would have been expected. However, the diminution is not linear, and the current decay is stepper than the linear relationship for the longer terraces. This fact indicates that AO molecules probably require more than one terrace site for their reduction. Another important fact that can be deduced is that peak currents for the Pt(n,n,n−2) electrodes are slightly higher than those obtained for the Pt(n+1,n−1,n-1) with comparable step density.

As has been demonstrated, the reduction of AO is extremely sensitive to the presence of (111) terraces, as it only takes place on the (111) terraces of the platinum. If so, the reduction currents measured for a polycrystalline platinum electrode should only contain the information regarding the (111) contributions present in the sample. Figure 7 shows the cyclic voltamograms of a polyoriented single crystal platinum bead in 0.5 M H_2SO_4 solutions before and after the addition of 0.01 M of AO. As can be seen, the voltammogram shows peaks at 0.14 and 0.19 V, typical for the reduction of the oxime on (111) terraces. Because the peak potential for the reduction of the oxime is sensitive to the terrace width, the response in this case is multiple because of the wide distribution of terrace (111) sizes present on the sample. On the other hand, in the positive scan, the reduction current is almost negligible, indicating that the fraction of wide (111) domains is very small and likely linked to the small facets present on the sample.

At this point, it is possible to propose AO reduction reaction as a potential test to determine the presence of (111) surface order domains for platinum nanoparticles. Three different samples with different nanoparticle shape have been studied. The voltammetric profiles of the nanoparticles samples in this study are shown in Fig. 8. The fraction of (111) and (100) ordered domains on those samples have been characterized by using bismuth and germanium irreversible adsorption, as proposed in references [21–23] (Table 1). These fractions correlate quite well with the shape of the nanoparticles observed by TEM. Thus, Pt1 sample is composed mainly by cubic nanoparticles, and as expected, the fraction of (100) ordered domains is very high. On the other hand, triangular-shaped nanoparticles predominate in Pt3 sample, having the higher ratio of (111) domains. Sample Pt2 has both types of nanoparticles and also some rounded particles. For that reason, the fractions of (111) and (100) sites have intermediate values. As can be seen, the observed reduction currents correlate quite well with the fraction of (111) sites present in the sample. Hence, Pt1 sample, for which the fraction of (111) sites is minimal, does not show any significant reduction peak for the oxime. As the fraction of (111) sites increases, the peak at ca. 0.16 V develops. It is also worth mentioning the presence of a well-marked reduction peak in the positive scan direction for the sample Pt3, a clear indication that the (111) domains present on the nanoparticles are relatively wide.

Conclusion

The AO reduction on the Pt(111) electrode and stepped surfaces after show a well-defined peak between 0.3 and 0.06 V vs RHE. Platinum surfaces without (111) terrace sites present a small and almost constant current in this potential range, which indicates that the oxime involved in the reaction only occur on the (111) terrace sites. Using the Pt(S)[n−1(111)×(110)] and Pt(S)[n(111)×(100)] stepped surfaces, it was found that the electrocatalytic process is dependent on the size of the (111) terraces, and moreover, the peak potential depends of the step site. Nanoparticles with different preferential shape were tested for the AO reduction reaction. The results are in agreement with those expected from the evaluation of the (111) ordered domains on the surface of the nanoparticles. The nanoparticles with (111) preferential orientation showed higher reduction

currents than the others, and the maximum of current strongly depends of the superficial order.

Acknowledgment This work has been performed in the framework of project CTQ2006-04071/BQU from MEC-FEDER (Spain).

References

1. Clavilier J, Parsons R, Durand R, Lamy C, Leger JM (1981) J Electroanal Chem 124:321
2. Lamy C, Leger JM, Clavilier J, Parsons R (1983) J Electroanal Chem 150:321
3. Adzic RR, Tripkovic AV, O'Grady W (1982) Nature 296:137
4. Adzic R (1990) Reaction kinetics and mechanisms on metal single-crystal electrode surfaces. In: White RE, Bockris JO'M, Conway BE (eds) Modern aspects of electrochemistry, vol. 21. Plenum, New York, pp 163–236
5. Markovic NM, Ross PN (1998) Electrocatalysis at well-defined surfaces: Kinetics of oxygen reduction and hydrogen oxidation/evolution on Pt(hkl) electrodes. In: Wieckowski A (ed) Interfacial electrochemistry, theory, experiments and applications. Marcel Dekker, New York, pp 821–842
6. Markovic NM, Ross PN (2002) Surf Sci Rep 45:117
7. Sriramulu S, Jarvi TD, Stuve EM (1998) Kinetic modelling of electrocatalytic reactions: methanol oxidation on platinum electrodes. In: Wieckowski A (ed) Interfacial electrochemistry, theory, experiments and applications. Marcel Dekker, New York, pp 793–804
8. Herrero E, Feliu JM, Aldaz A (2003) Electrocatalysis. In: Bard AJ, Stratmann M (ed) Encyclopedia of electrochemistry, vol. 2. Wiley-VCH, Weinheim, Germany, pp 443–466
9. Koper MTM, Van Santen RA, Neurock M (2003) Theory and modelling of catalytic and electrocatalytic reactions. In: Wieckowski A, Savinova ER, Vayenas CG (ed) Catalysis and electrocatalysis at nanoparticle surfaces. Marcel Dekker, New York, pp 1–34
10. Vidal-Iglesias FJ, García-Aráez N, Montiel V, Feliu JM, Aldaz A (2003) Electrochem Commun 5:22
11. Ahmadi TS, Wang ZL, Green TC, Henglein A, El-Sayed MA (1996) Science 272:1924
12. Petroski JM, Wang ZL, Green TC, El-Sayed MA (1998) J Phys Chem 102:3316
13. Narayanan R, El-Sayed MA (2004) J Phys Chem B 108:5726
14. Pierozynski B, Conway BE (2002) J Electroanal Chem 538-539:87
15. Baizer MM, Lund H (1983) Organic electrochemistry. An introduction and a guide. Marcel Dekker, New York
16. Clavilier J, Armand D, Sun S-G, Petit M (1986) J Electroanal Chem 205:267
17. Herrero E, Orts JM, Aldaz A, Feliu JM (1999) Surf Sci 444:259
18. García-Aráez N, Climent V, Herrero E, Feliu JM (2004) Surf Sci 560:269
19. Solla-Gullón J, Montiel V, Aldaz A, Clavilier J (2000) J Electronal Chem 491:69
20. Solla-Gullón J, Rodes A, Montie V l, Aldaz A, Clavilier J (2003) J Electroanal Chem 554:273
21. Rodríguez P, Herrero E, Solla-Gullón J, Vidal-Iglesias FJ, Aldaz A, Feliu JM (2005) Electrochim Acta 50:3111
22. Rodríguez P, Herrero E, Solla-Gullón J, Vidal-Iglesias F, Aldaz A, Feliu JM (2005) Electrochim Acta 50:4308
23. Rodríguez P, Solla-Gullón J, Vidal-Iglesias F, Herrero E, Aldaz A, Feliu JM (2005) Anal Chem 77:5317
24. Albalat R, Claret J, Rodes A, Feliu JM (2003) J Electroanal Chem 53:550–551
25. Rodríguez-López M, Herrero E, Feliu JM, Tuñón P, Aldaz A, Carrasquillo A (2006) J Electroanal Chem 594:143
26. Gómez R, Orts JM, Rodes A, Feliu JM, Aldaz A (1993) J Electroanal Chem 358:287
27. Climent V, Rodes A, Orts JM, Feliu JM, Aldaz A (1997) J Electroanal Chem 436:245
28. Climent V, Rodes A, Orts JM, Feliu JM, Aldaz A (1999) J Electroanal Chem 467:20
29. Gómez R, Climent V, Feliu JM, Weaver MJ (2000) J Phys Chem B 104:597